EUROPEAN JOURNAL OF COMPUTER SCIENCES AND INFORMATICS
2026; 3(2): 67-82.
10.5455/EJCSI.20251213060931

WisdomGale

ORIGINAL ARTICLE

Open Access

Resource-efficient conjunctivitis screening using MOGONET and VGG-based transfer learning

Pranto Halder[1], Anurag Sinha[2], Khalid Hasan[3], Amit Kumar[4], Jibran Gulzar[5], Anmol Chauhan[6], Divyank Sharma[7], Pratyush Singh[8], Sagar Singh[9], Kshitij Tandon[10], Kshitij Ranjan[11], Aditya Pandey[12]

[1]Computer Science and Engineering, Faculty of Science and Engineering, Teesta University, Rangpur, Bangladesh

[2]ICFAI Tech School, ICFAI University, Ranchi, India

[3]Electrical and Electronic Engineering, Faculty of Science and Engineering, Teesta University, Rangpur, Bangladesh

[4]Computer Science, Engineering Rungta College of Engineering & Technology, Bhilai, India

[5]Computer Science and Engineering, Kalasalingam Academy of Research and Education, Virudhunagar, India

[6]Department of Computer Science and Engineering, CSPIT, Charotar University of Science and Technology (CHARUSAT), Changa, India

[7]Department of Computer Science and Engineering, Sharda University, Greater Noida, India

[8]Department of Computer Science and Engineering, Sharda University, Greater Noida, India

[9]ABES Engineering College, Ghaziabad, India

[10]Department of Computer Science and Engineering, Jaypee University of Engineering and Technology, Guna, India

[11]Computer Science and Data Analytics, IIT Patna, Patna, India

[12]Department of Electronics and Computer Engineering, National Institute of Advanced Manufacturing Technology, Ranchi, India

ABSTRACT

Background/Aim: Conjunctivitis, commonly known as pink eye, poses a significant diagnostic challenge due to overlapping presentations across viral, bacterial, and allergic subtypes. This study presents MOGONET, a multi-objective generalized normal distribution optimization framework built upon VGGNet, specifically designed to address conjunctivitis identification through resource-aware deep learning optimization.

Methods: The proposed pipeline integrates contrast-limited adaptive histogram equalization-based image enhancement, data augmentation, and multi-level Otsu thresholding segmentation with transfer learning using a VGG16 backbone. A MOGNDO-based outer-loop search simultaneously maximizes classification accuracy, minimizes binary cross-entropy loss, and minimizes computational cost (FLOPs) using Pareto-front-based non-dominated sorting. Experiments were conducted on 1,230 conjunctival eye images sourced from Kaggle and Shutterstock, with a stratified 72%/18%/10% train/validation/test split.

Results: MOGONET achieves 98.32% test accuracy, 97.54% precision, 96.92% recall, and 96.22% F1-score. Compared with the unoptimized Visual Geometry Group-based baseline, MOGONET reduces FLOPs by 79.18% (from 238.06M to 49.56M), and model parameters by 77.78% (from approximately 9M to 2M).

Conclusion: MOGONET demonstrates that multi-objective optimization can substantially reduce computational complexity in conjunctivitis classification without sacrificing diagnostic performance, offering a promising framework for deployment on resource-constrained clinical screening platforms.

ARTICLE HISTORY

Received December 13, 2025
Revised March 12, 2026
Accepted March 12, 2026
Published April 13, 2026

KEYWORDS

Conjunctivitis; generalized normal distribution optimization; multi-thresholding, deep learning

Contact Pranto Halder ✉ prantohalder117@gmail.com Computer Science and Engineering, Faculty of Science and Engineering, Teesta University, Rangpur, Bangladesh

© The Author(s) 2026. Open Access This article is licensed under a Creative Commons Attribution 4.0 International License (CC BY). http://creativecommons.org/licenses/by/4.0/.

Introduction

Conjunctivitis, commonly referred to as pink eye, is a widespread cause of ocular redness and can impact individuals across all age groups and socioeconomic strata. Conjunctivitis caused by viruses is the predominant etiology of infectious conjunctivitis, accounting for about 75% of cases [1]. The three principal causes of conjunctivitis are infectious, hypersensitive, and microbiological variables, with adenovirus accounting for the most of cases. Conjunctivitis causes the eye to appear red because of vasodilation and is usually accompanied by increased lacrimation and/or mucus discharge. This can elevate the probability of viral conjunctive inflammation along with the procedures for evaluating and managing the ailment. It emphasizes the significance of a coordinated medical group in enhancing the quality of treatment for patients with epidemiologic conjunctivitis. Moreover, medical practitioners find it difficult to differentiate between pathological and bacteriological conjunctivitis, prompting them to take a conservative approach and prescribe antibiotics as a preventive step. The lack of a conclusive analysis is a well-acknowledged feature leading to the over medicament of suppository for upper respiratory infections [2]. In this environment, bacterial illnesses are constructed on medical criteria, and the possible hazard of rare complications is highly problematic. For screening tools to be effective, specialists must perform manual reviews of images to recognize infections. The cost of developing operational screening is substantial because to the complex environment of the analysis and the scarcity of qualified personnel. Current automated approaches, despite their efforts, are incapable of properly managing a wide range of diseases and real-world scenarios [3].

Novelty and positioning

This paper proposes MOGONET, a resource-aware multi-objective optimization framework for conjunctivitis identification that adapts the Multi-objective Generalized Normal Distribution Optimization (MOGNDO) strategy to CNN design and training. In contrast to standard multi-objective evolutionary algorithms (e.g., NSGA-II), MOGONET couples GNDO-based sampling/updating with an archive of non-dominated solutions and explicitly encodes CNN architecture and training choices (e.g., input resolution, convolutional filter configuration, and classifier head) to jointly (i) maximize validation accuracy, (ii) minimize validation loss, and (iii) minimize computational cost (FLOPs). The underlying GNDO/MOGNDO operators are retained; the contribution lies in the problem formulation, FLOPs estimation within the learning pipeline, and integration with a Visual Geometry Group-based transfer-learning (TL) model for conjunctivitis.

The utilization of deep learning (DL) in healthcare image assessment markedly improves disease detection and diagnosis. Earlier scientific approaches for disease identification were less reliable, prone to misdiagnosis, and often necessitated considerable time to obtain appropriate results. Recently, the biomedical field has widely embraced machine learning techniques for disease detection, producing very accurate results in a short period. The aim of this study is to develop a model employing image processing and DL methods to assess the identification of conjunctival eye disorders. Optimization procedures are esteemed as effective strategies for identifying optimal mainframe strategies. The vast majority of estimated strategies are broad search methodologies referred to as meta-heuristics.

These strategies are designed to mitigate the deficiencies of traditional methodologies. In recent decades, numerous metaheuristic procedures encouraged by natural spectacles, combined conduct, and systematic ideologies have been presented, containing bald and golden eagle, ant colony, dynamic arithmetic, grey wolf, and particle swarm optimization which are categorized as computational-based processes adhering to the principles of mathematics and physics [4]. Research demonstrates that metaheuristic algorithms can deliver highly accurate solutions to complicated optimization problems within a reasonable timeframe. Metaheuristic algorithms offer advantages over analytical techniques, including affluence of execution, a straightforward context, commendable precision, and acceptable performance time. Confronting real-world issues entails various challenges that require the utilization of particular techniques. Multi-objectivity is a fundamental attribute of real-world problems that complicates their resolution. A challenge involving the enhancement of numerous objectives is termed multi objective issues.

Clearly, several objective optimizers must be employed to address such problems. Since then, a significant array of studies has been dedicated to developing multi-objective evolutionary and heuristic algorithms.

The implementation of stochastic optimization techniques in practical situations has been facilitated by the use of gradient-free approaches and schemes that avoid entrapment in an indigenous ideal situation. Multi-objective optimization methodologies are currently employed across diverse domains. Numerous single-objective methodologies that have been established can also be employed to tackle multi-objective optimization challenges. The GNDO, newly introduced by Zhang et al. [5], is acknowledged for its effectiveness in worldwide identifying optimal solutions for single-objective optimization problems. A preliminary examination of relevant literature indicates that GNDO has effectively addressed intricate optimization problems in various domains. This multi-objective method demonstrates enhanced performance relative to current techniques. This may result from the integration of novel methods, optimization approaches, and procedures. The outcome can enhance the system's applicability in real-life scenarios.

An advanced DL approach that integrates TL to precisely identify conjunctive disorders in the eyes is proposed, thereby addressing the aforementioned problems. This study utilizes histogram equalization to enhance the local contrast of a designated area, subsequently applying the Contrast-Limited Adaptive Histogram Equalization (CLAHE) technique, which serves as a contrast limitation method to avoid the unnecessary intensification of blare and artifacts in conjunctive eye image samples. Additionally, multi-objective optimization procedures incorporate numerous diverging objectives, unlike single-objective optimization, which includes accuracy, loss, model cost, and algorithm complexity, while striving to enhance network efficiency and performance [6–22]. To evaluate a MOGNDO algorithm integrated with the VGGNet CNN model with the defined objectives, followed by the formulation of the GND and the development of the optimization process. The proposed methodology integrates the MOGNDO structure with the VGGNet framework to improve hyperparameter

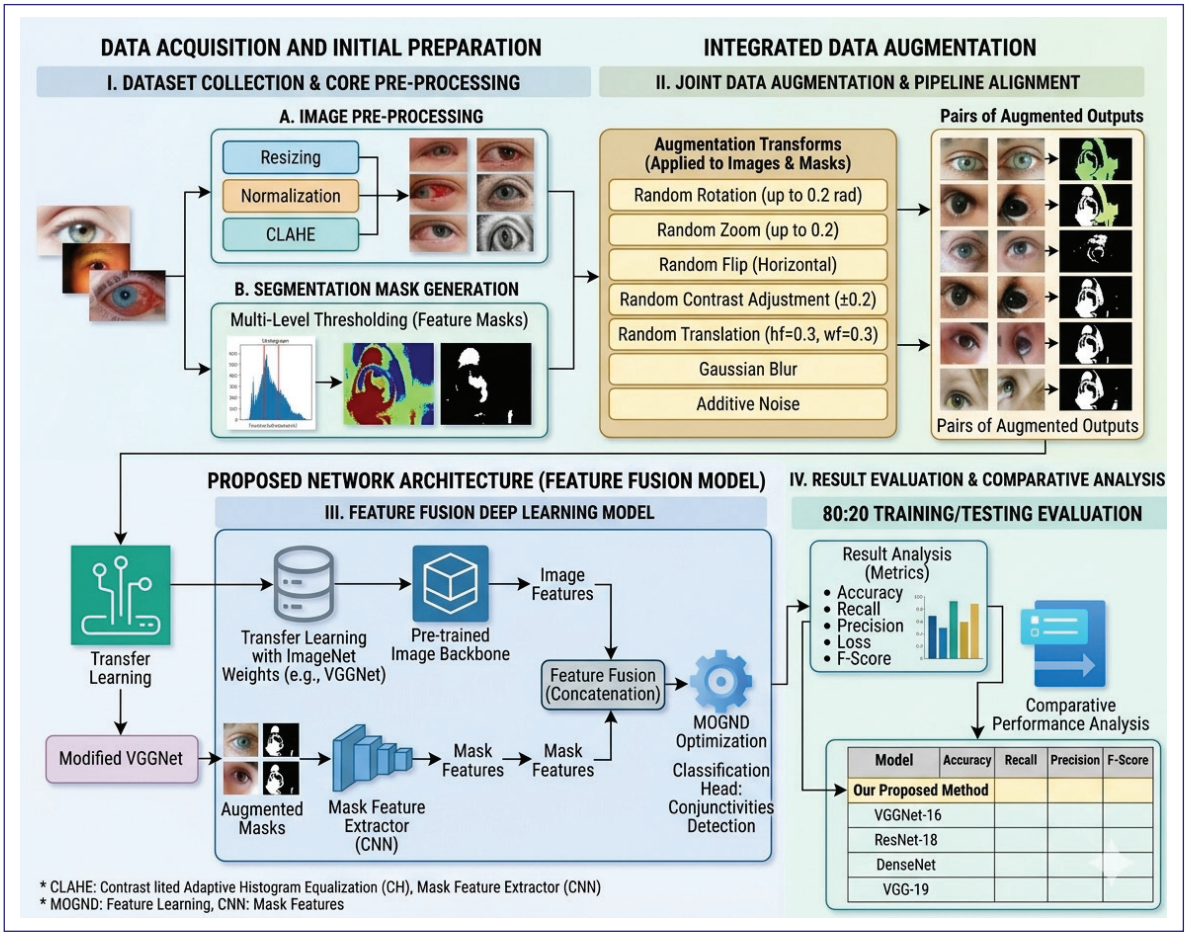


Figure 1. Overview of the proposed MOGONET-based workflow for conjunctivitis detection, including dataset acquisition, image pre-processing and augmentation, multi-level Otsu-based segmentation, VGG16-based transfer learning, and multi-objective optimization for final classification.

Table 1. Dataset specification.

Specification	Value
Dataset Sources	Kaggle and Shutterstock conjunctivitis datasets
No. of classes	2
Classes	Conjunctivitis, Healthy
Health images	422
Conjunctivitis images	808
Total images	1,230
Images after data augmentation	11,070
Training data	7,970
Validation data	1,993
Test data	1,107

Table 2. Data-augmentation function.

Functions	Values
Random Flipping	Horizontal
Random Translation	(HeightFactor = 0.1, WidthFactor=0.1)
Random Rotation	(20^0 and 30^0)
Random Zoom	(HeightFactor = 0.4, WidthFactor=0.4)
Brightness	50%
contrast	50%
Gaussian Blur	Sigma(0.1,2.0),kernel size = 5
Add Noise	Gaussian noise

optimization. By integrating MOGNDO with the VGGNet framework, the hyperparameters and other variables of the VGGNet model employed for image classification can be optimized. This technique simultaneously improves multiple conflicting objectives, including model accuracy, complexity, parameter count, computational cost, and memory consumption, while also reducing the training time required for the model.

The paper is organized as follows: the Introduction presents the clinical background and motivation. Materials and Methods details the dataset, preprocessing pipeline, VGGNet16 model, and MOGNDO optimization framework. Results present quantitative performance evaluations. The Discussion interprets the findings in context. The Conclusion summarizes contributions and future directions.

Materials and Methods

The pre-processing enhances the dataset's overall image quality by the application of numerous image processing approaches. Moreover, data augmentation is employed to reduce the likelihood of the system demonstrating over-fitting. As a result of the technique used a significant rise in the overall number of collected datasets. The enhanced segmentation approach describes the utilization of meta-heuristic procedures within the multilevel thresholding framework, utilizing Otsu's method. The retrieving attributes and classification module delineates the proposed model utilized for

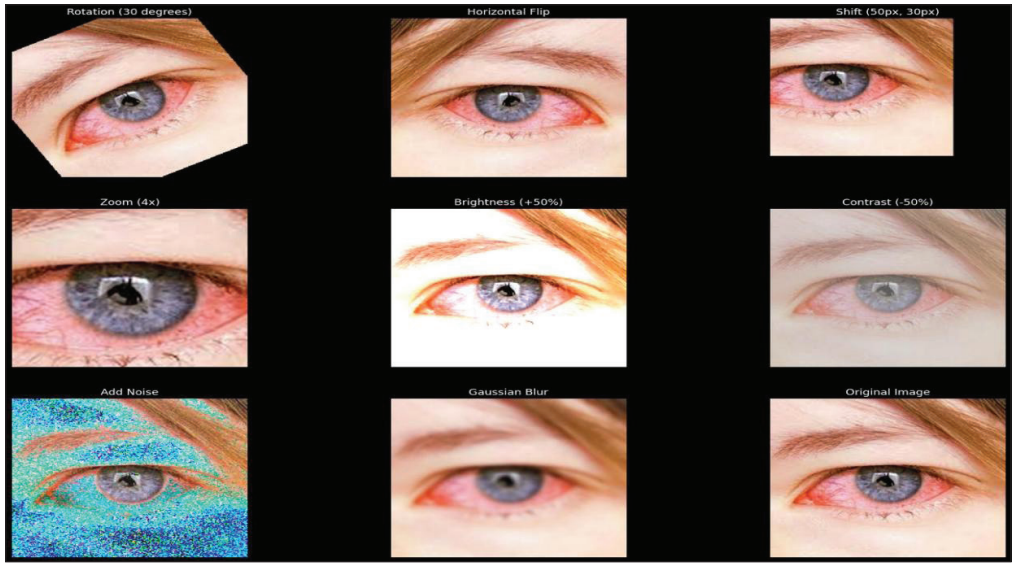


Figure 2. Class distribution of the conjunctivitis dataset and the corresponding stratified train, validation, and test split used in this study.

discerning the classification of conjunctival eye illnesses using DL with TL. Figure 1 illustrates the graphic illustration of the work stream for the study. The dataset section is now initiating the study's methodology, which will sequentially address the primary elements of the proposed work.

Dataset and image processing

Shutterstock and Kaggle conjunctiva datasets are employed [23,24]. The collection comprises nearly 800 image samples with conjunctivitis and 430 healthy eyes images samples. Feature selection strategies are essential for enhancing the attributes of the learning module. Unadjusted data present a difficulty for formations and substantially impede the predicting efficacy of various machine learning methods. This type of statistic also affects and can even obstruct the association of numerous gradient-centered estimation methods. We utilized a rescaling procedure for each image in this specific instance. It enhances the performance of CNN models by the incorporation of augmentation techniques. Nine factors have been used to improve the training and testing samples of the conjunctive eyes' datasets. The standards include Horizontal Flip, Translation, Random Contrast, Random Rotation, Gaussian Blur, and Random Zoom [25]. Figure 2 illustrates the dataset class distribution and data split. Figure 3 illustrates the outcome of the image augmentation procedure subsequent to the implementation of several utilities. Table 1 represents the specification of image sample used for the study. Table 2 represents the function parameter of the data augmentation function applied on image samples.

Algorithm 1. Pre-processing and segmentation of conjunctive eye.

Input: ConjEye Samples $\{X = x_{1,}x_{2,}x_{3}\ldots\ldots\ldots\ldots\ldots x_{n}\}$ where n is image count.
Output: Multi-threshold Segmented Images {Ɨ$_s$ = i_1, i_2, i_3……, $i_{m,}$} where Conjunctive Eye segmented image *i*.

1. Load the image dataset, take image from dataset, and convert the image to grayscale using φ (Ļ) =
2. Apply CLAHE: Calculate $\hat{h}_l(i), \text{and}\,\hat{h}(j)$, "hologram" i ∈ {1,2,...,ť} and 'ť' is the total number of tiles,
3. Clip the histogram $H_l(j)$ with 8 × 8-tile grid and a clip limit of 2.0. and Redistribute the clipped pixel intensities among the other bins in the histogram $H_l(j)$ to obtain equalization.
4. Utilize the method of bilinear interpolation to amalgamate histograms that consist of adjacent tiles and replace the original conjunctive eye image x_i in the samples with the contrast-enhanced images and return {$Q = q_{1,}$ $q_{2,}$ q_3 ……q_i} dataset.

1. Read the contrast-enhanced image dataset Ɨ$_s$ and generates Bi-level thresholding image be represented by

$$\beta(m,n)=\begin{cases}\alpha_{1<-^2(m,n)\,\text{if}\,0\le{}^2(m,n)<\text{Threshold}\,\check{T}}\\ \alpha_{2<-^2(m,n)\,\text{if Threshold}\,\check{T}\le{}^2(m,n)<t-1}\end{cases}$$

where, β(m,n) I bi-level image having size (m,n) with Ļ intensity level, α_1 & α_2 are two categories depend on the threshold value Ť.

2. Apply fitness function considering multi-level threshold value f_{ost} (Ť$_i$)= Θ = aggregate (max(Ť$_k$)) 0≤ Ť$_k$ ≤ *l*–1
3. Calculate shanon entropy $S_H = \sum_{k=1}^{\eta} P_k \log_2 P_k$ where η is the number of the pixel, P_m is the probability of kth gray level, P_m *is the probability of kth gray level* {$P_k = p_1, p_2, p_3$……..p_k}, shows the probable distribution of the grayscale levels.
4. Find optimal threshold value $\Phi_k = \ln p_\eta\left(1-p_\eta\right)+\dfrac{\left(H_\eta - H_k\right)p_k + H_k\left(1-p_k\right)\right)}{p_k\left(1-p_k\right)}$, while entropy function maximizes posterior entropy, Otsu maximizes the in class dispersion.
5. AOA exploration operators analyses the entire image using several zones determined by adjusted Otsu values in order to find a more effective solution, and following the initial phase, there is a continual sequence of outcomes that persist until the optimization procedure is accomplished.
6. Replace the original conjunctive eye segmented image q_i in the dataset with the segmented image and return {Ɨ$_s$ = i_1, i_2, i_3……i_m} dataset.

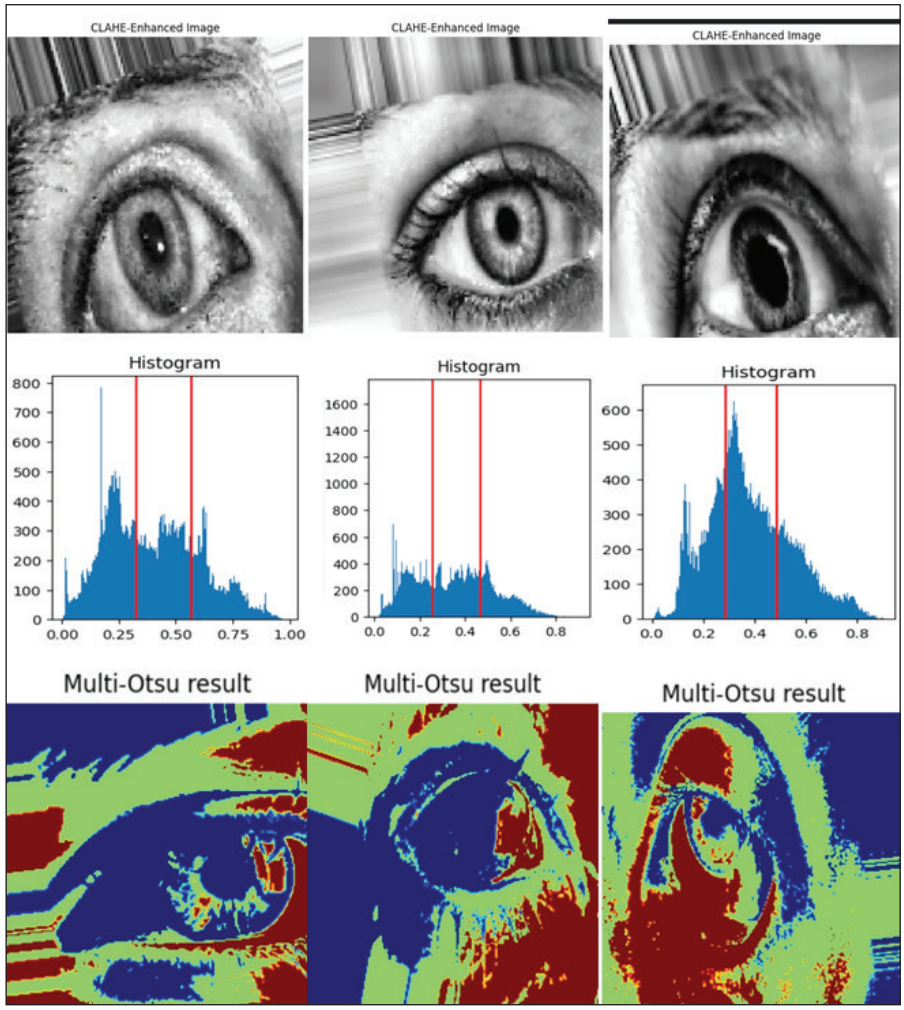


Figure 3. Representative pre-processed and segmented conjunctival eye images used in the proposed framework.

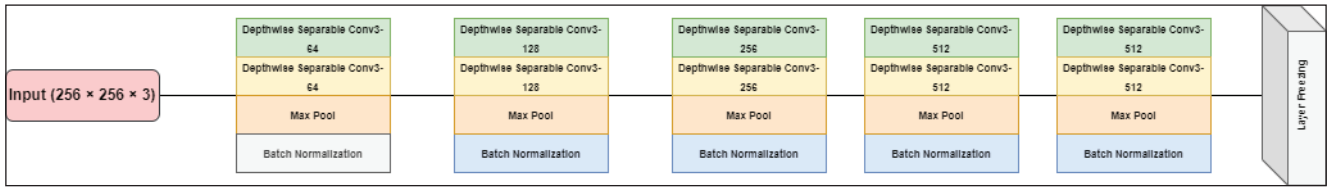


Figure 4. Representative pre-processed and segmented conjunctival eye images used in the proposed framework.

Dataset integrity and split protocol: Images were collected from public web sources (Kaggle and Shutterstock). To reduce leakage risks from near-duplicate or visually similar images, we screened and removed duplicates prior to splitting (exact duplicates via file hashing, and near-duplicates via perceptual hashing with manual review). We then created a single stratified train/validation/test split at the level of the original images (72%/18%/10% per class). All derived variants (pre-processed, segmented, and augmented versions) inherited the split of their corresponding original image to prevent cross-split leakage. Labels follow the annotations provided by the source repositories and therefore reflect visual labeling rather than clinically verified patient records. The final processed sample counts are reported in Table 1. The dataset comprises two classes: conjunctivitis (808 images, 65.69%) and healthy eyes (422 images, 34.31%), for a total of 1,230 original images. Figure 2 provides a visual overview of the class distribution and the train/validation/test split proportions. MOGONET performs binary classification (conjunctivitis vs. healthy) using a sigmoid output activation

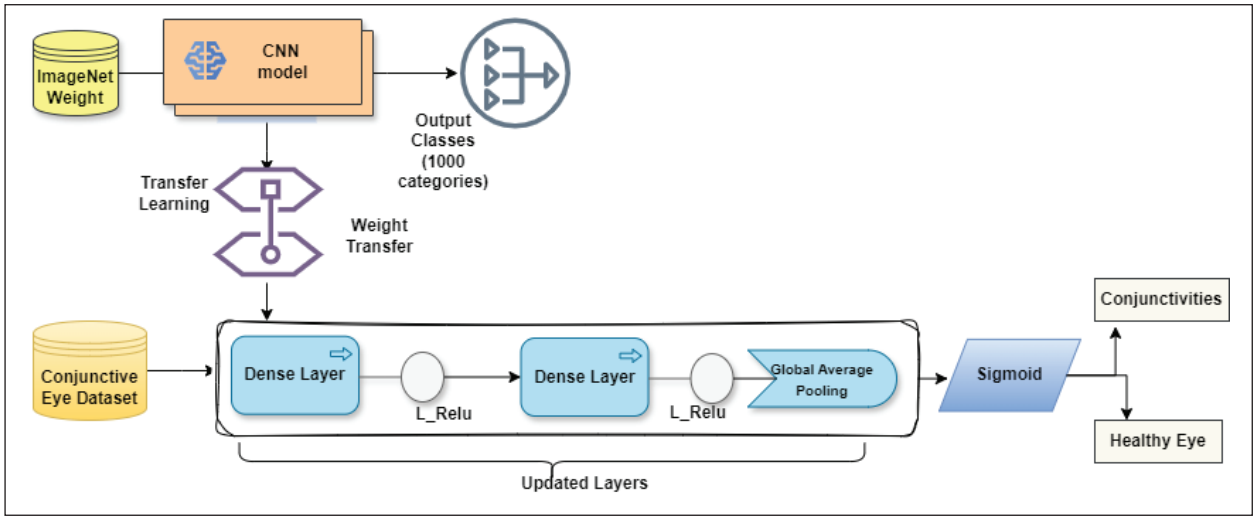


Figure 5. Representative feature maps extracted by the proposed VGG16-based model.

with a decision threshold of 0.5; severity sub-levels are not modeled in the current framework. Readers interested in severity-level detection are directed to ConjunctiveNet [26].

This section presents a method for improving medical images of the conjunctiva by integrating normalization and CLAHE techniques. The proposed scheme enhances disparity and reduces noise for the RGB constituents of the input samples [27]. An endeavor is undertaken to rectify the inconsistency in quality metrics that arises while implementing noise lessening and contrast enhancement across all channels of the input image. The multi-level thresholding methodology utilizes heuristic algorithmic techniques, specifically the modified Otsu's method [28]. Threshold determined from Ostu's method with the highest inconsistency ratio for each individual group. The efficacy of the novel independent utility is assessed in comparison to the established entropy and Otsu's roles to ascertain the ideal multi-level thresholding range requisite for segmenting AOA approaches. Each distinct region intimates an image has an exclusive inception defined by its particular attributes. The approach of segmenting digital images by histogram thresholds is largely acknowledged as the maximum deployed technique. The automated image segmentation and their associated framework is a vigorous and engaging domain within feature extraction and classification. Furthermore, it possesses the potential to provide distinct forecasts or perform initial data modification for more complex phases. Algo. 1 delineates thresholding as bi or multi-level, depending upon the requisite threshold values for image segmentation. Bi-level thresholding splits an image into two separate areas, while multi levels generate several districts inside a single image. The modified Otsu's approach can be utilized for the conjunctivitis dataset. Algorithm 1 delineates the sequential procedure utilized in the improved multi-level thresholding. Figure 3 illustrates the improvement of the image within the pre-processing context with pre-processing and segmentation.

MOGONET model and optimization

The proposed methodology integrates the MOGND structure with the VGGNet framework to improve hyperparameter optimization. By integrating the MOGND with the VGGNet framework, the hyperparameters and other variables of the VGGNet model employed for conjunctivitis classification can be optimized. This section outlines the sequential techniques utilized by the proposed MOGONET technology.

VGGNet16

The VGGNet16 model is utilized 4096 features from each area application. VGGNet is regarded as the most sophisticated and effective framework for classification chores. It is utilized for TL due to its adaptability for various tasks. VGGNet comprises 16 layers, each possessing individual weights. The network was modified by removing the last three levels for categorization purposes. Mean-subtracted 256 × 256 images undergo processing through 5 convolutional layers followed by 2 fully connected dense layers to generate statistics [29]. In contrast, Figure 4 depicts the essential structural framework of the proposed work. The procedure integrates the attributes of VGGNet while utilizing a modified DL

Algorithm 3. MOGONET.

Input: Dataset $\{Ł_s = i_1, i_2, i_3 \ldots\ldots\ldots\ldots i_m\}$ and initial population $^{(0)}$ with predefined parameters

Output: Optimized MOGONET model solution space { for conjunctivitis classification.

1. **Initialization of** randomly generated **candidate solutions of VGGNet variants, including** learning rate ϑ_1 , no. of filtersϑ_2, batch sizeϑ_3, dropout rate $\vartheta_3$and other hyperparameters $\vartheta_4$using **GND**.

Initial population $^{(0)}$ with predefined parameters $\alpha^{(0)}$, $\beta^{(0)}$, $\gamma^{(0)}$.

$$\boldsymbol{\mathcal{P}}^{(0)} = \{\vartheta_1^{(0)}, \vartheta_2^{(0)}, \vartheta_3^{(0)} \ldots \vartheta_n^{(0)}\}$$

2. For each VGGNet candidates solution $\vartheta_i^{(k)}$ in the $\boldsymbol{\mathcal{P}}^{(0)}$ in generation k, objective functions are calculated on segmented image dataset of conjunctivitis after training the VGGNet model:

$$\varphi 1($$

$$\varphi 2($$

$$\varphi 3($$

Above objectives are typically conflicting representing accuracy, FLOPs, and loss.

3. Perform front and non-dominated sorting to recognize pareto front consisting of non-dominated solutions that depicts the trade-off between the objectives.

$$\varphi n($$

$$\varphi n(\text{for at least one n}$$

4. Updating the GND parameter $\alpha^{(k+1)}, \beta^{(k+1)}, \gamma^{(k+1)}$ based on pareto front for the next generation using:

$$\alpha^{(k+1)} = \frac{1}{Z}\sum_{i=1}^{Z}\left(\vartheta_i^{(k)}\right)$$

$$\beta^{(k+1)} = \sqrt{\frac{1}{Z}\sum_{i=1}^{Z}(\vartheta_i^{(k)} - \pm^{(k+1)})^2}$$

$$\gamma^{(k+1)} = \textit{update shape parameter relied on performance}$$

5. Now, generate the new updated population $\boldsymbol{\mathcal{P}}^{(k+1)}$ of the VGGNet model's candidate solution from updated GND:

$$\boldsymbol{\mathcal{P}}^{(k+1)} = \{\vartheta_1^{(K+1)}, \vartheta_2^{(K+1)}, \vartheta_3^{(K+1)} \ldots \vartheta_n^{(K+1)}\}$$

$$\text{For each} \in \text{GND}\left(\vartheta_i^{(K+1)} \in \alpha^{(k+1)}, \beta^{(k+1)}, \gamma^{(k+1)}\right)$$

6. Repeat steps 3, 4 and 5 until the convergence criterion is met and pareto front will get the solution $\{\vartheta_1^*, \vartheta_2^*, \vartheta_3^* \ldots \vartheta_n^*\}$ representing different trade off among the objectives and each solution provides the optimized VGGNet model for a specific balance of accuracy, complexity, and computational cost.
7. Evaluate the $Model_{finetune}$ on the testing set $Ł_{test}$ with "accuracy", "precision", "Recall", F-score, specificity, and loss.
8. Save the optimized Basis MOGONET model for future use in detecting the conjunctive eyes classification tasks.

technique. The initial phase entails recognizing the fundamental nets of the TL procedure and assigning the network weights utilizing the pre-trained deep model. Subsequently, lowest layers of the structure are altered to reconstruct its architecture. This method facilitates the attainment of a new and modified model formation. Successively, the newly created framework can be refined by modifying their factors to diminish the loss utility, employing the available inputs and associated labels. Optimizer SGD is utilized to compute the optimum weights though managing the loss, expressed as

Table 3. Parameters of MOGONET.

Parameter	Values
Train/Validation ratio (within development set)	80:20
Optimizer	stochastic gradient descent
I/P Image size	100 × 100, 128× 128, 256 × 256
Epochs	50
Learning rate	0.001
Output activation Function	Sigmoid
Batch size	64
Pretrained Parameters	ImageNet
momentum	0.9
Total iterations	100
Language and Package	Python with TensorFlow/Keras and OpenCV
Train/Validation/Test split (stratified, group-wise)	72% / 18% / 10%
Random seed	42
Runs	Single run (fixed split)

Table 4. Experimental results.

Model	Accuracy (%)	FLOPs	Loss	Params
VGGNet 16	93.48	311.53 M	0.325	≈ 15 M
VGGNet 19	91.62	397.31 M	0.613	≈ 20 M
ResNet 50	89.73	1311.05 M	0.258	≈ 23 M
DenseNet	87.02	289.21 M	0.581	≈ 2 M
ResNet18	91.49	535.41 M	0.326	≈ 12 M

sparse cross-entropy. The recommended MOGONet system is an enhanced version of the VGGNet-16 architecture with optimization module. The TL procedure was employed to transform it into a attribute retriever, thereafter augmented by the addition of three supplemental layers to improve the DL architecture. Ultimately, the model succeeded in executing its newly designated mission. The Global_Avg_Pooling with two compact layers have been modified to maximize outcome. It is executed to achieve the goal of optimum results. Figure 5 illustrates the proposed design that employs TL. A sigmoid function is utilized for the binary classification of conjunctive disease. The novel model consists of two primary components: the initial segment is the pre-trained model, and the subsequent element comprises the extended layers utilized on a multiscale feature generation for binary class classification.

Multi-objective generalized normal distribution optimization

In the following subsection, the GNDO technique is presented. It intended for addressing multi-objective optimization challenges, is defined and brought forward in the study [30]. Finally, the operational overhead of MOGONET is recommended.

Generalized normal distribution optimization

The proposed strategy achieves a balance between both exploration and extraction through multiple approaches. The process of exploring in solution-based approaches generally comprises three essential parts. At the beginning, each initial solution is widely distributed. Subsequently, such solutions progress toward the optimal solution, directed by certain investigating and refining methodologies. Ultimately, all convergence on the optimal solution is identified. The way it works could be elucidated through numerous normal distributions, with the position of every outcome seen as a variable according to a normal distribution. Initially, the mean position and the optimal location are significantly far, and the dispersion of all solution locations is considerable. As searching advances, the disparity between the average site and the optimal location diminishes, and the variability in locales reduces. In the concluding phase, either the length from the mean to the optimal position and the variability in solution positions are eliminated. GND presents a clear structure, with its sharing information methods consisting of local extraction and global investigation. Exploitation utilizes a GND model, guided by the current average and ideal placements. Simultaneously, exploring entails the random selection of three persons. The approach commenced with the establishment of a random sample.

Objective evaluation

The recommended MOGONet concurrently maximizes the accuracy of classification and FLOPs, loss; thus, in the goal-oriented assessment of MOGONet. All metrics are computed and presented as the goals of the user outlined in Algorithm 3 (MOGONET). To ascertain the precision of classification, the dataset is partitioned into training and test subsets prior to training the VGGNet model with designated hyperparameters. The model is trained on the training subset and subsequently

Table 5. Experimental results of Benchmark CNN models.

Model	Acc (%)	ΔAcc (pp)	FLOPs	ΔFLOPs (%)	Loss	ΔLoss (%)	Params	ΔParams (%)
VGGNet 16	93.48	—	311.53 M	—	0.3256	—	≈ 15 M	—
Multi objective optimization VGGNet 16	92.51	−0.97	57.84 M	81.43%	0.1512	53.56%	≈ 3 M	80.00%
VGGNet 19	91.62	—	397.31 M	—	0.6137	—	≈ 20 M	—
Multi objective optimization VGGNet 19	91.89	0.27	132.11 M	66.75%	0.3824	37.69%	≈ 9 M	55.00%
ResNet 50	89.73	—	1311.05 M	—	0.2587	—	≈ 23 M	—
Multi objective optimization ResNet 50	91.66	1.93	542.79 M	58.60%	0.0699	72.98%	≈ 11 M	52.17%
DenseNet	87.02	—	289.21 M	—	0.5817	—	≈ 2 M	—
Multi objective optimization DenseNet	86.71	−0.31	127.31 M	55.98%	0.2793	51.99%	0.2 M	90.00%
ResNet18	91.49	—	535.41 M	—	0.3268	—	≈ 12 M	—
Multi objective optimization ResNet18	92.04	0.55	113.68 M	78.77%	0.2031	37.85%	≈ 8 M	33.33%
Proposed Model without MOO	96.88	—	238.06 M	—	0.2179	—	≈ 9 M	—
Proposed MOGONET	98.32	1.44	49.56 M	79.18%	0.0193	91.14%	≈ 2 M	77.78%

Table 6. Image resizing outcomes.

Image size (Proposed Model)	Acc (%)	FLOPs	Loss	Params
100 × 100	96.46	31.72 M	0.0,1256	≈ 1.9 M
128 × 128	98.21	41.84 M	0.0,1512	≈ 1.7 M
256 × 256	98.32	49.56 M	0.0,193	≈ 2 M
512 × 512	95.41	92.23 M	0.1,948	≈ 11 M

evaluated on the test subset utilizing a backpropagation algorithm with the Adam optimization method. The optimization objective of the suggested MOGONet is to enhance classifying accuracy the FLOPs are computed for the individual, serving as the secondary objective, and the suggested MOGONET aims to reduce the FLOPs count. Nextly, to reduce the training loss of the model is the third objective as stated below.

Obj-1: Maximization of accuracy

The accuracy of the model can be optimised by balancing the other objectives using MOGONET optimization approach

$$\mathrm{acc}\left(\vartheta_i^{(k)}\right)=\frac{1}{Z}\sum_{i=1}^{Z}\varphi(a_i(\vartheta),\tilde{a}_i) \tag{1}$$

where, $\mathrm{acc}\left(\vartheta_i^{(k)}\right)$ is the accuracy function on VGGNet parameters ϑ, $\tilde{a}_i(\vartheta)$ is the predicted value, and Z is the total number of conjunctive eye samples

$$\varphi\left(\tilde{a}_i(\vartheta),\tilde{a}_i\right)=\begin{cases}1 & if\ a_i=\tilde{a}_i\\ 0 & otherwise\end{cases} \tag{2}$$

The objective function of maximization of accuracy is to fine-tune the VGGNet parameters ϑ to improve $\mathrm{acc}\left(\vartheta_i^{(k)}\right)$.

Obj-2: Minimization of FLOPs

The floating-point operation per second (FLOPs) in VGGNet relied on different factors such as filter count layer count and image size. To optimize the computational complexity of a VGGNet model need to be minimized FLOPs without compromising the model's accuracy. FLOPs in the convolutional layers can be calculated as

$$\mathrm{FLOPs}=2\times(OFM_{\mathrm{height}}\times OFM_{weight})\times(Ch_{\mathrm{in}}\times K\times k)\times Ch_{\mathrm{out}} \tag{3}$$

where OFM_{height} and OFM_{weight} is output feature map for height and width dimensions, Ch_{in} is input channels count, and ch_{out} is output channel count or

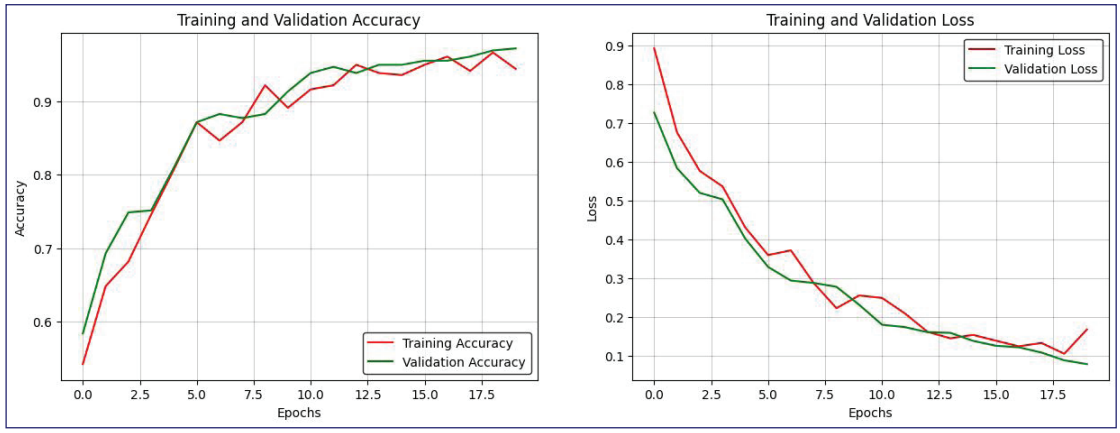


Figure 6. Transfer-learning architecture of the proposed MOGONET model for conjunctivitis classification.

filter count, K × k is the kernel size of the VGGNet. For the fully connected layers number of FLOPs can be computed as follows:

$$Dense\ FLOPs = 2 \times (\eta_{in} \times \eta_{out}) \quad (4)$$

The FLOPs can be reduced without compromising the accuracy by Different techniques like reducing the filter count in the convolutional layer, number of layers can be reduced in order to decrease the FLOPs, image size also effects the FLOPs count; and different techniques like pruning, quantization, and depth wise separable convolutions can be utilized. However, this might decrease the accuracy of the network due to representational power of model can be minimized. MOGONET technique will let to solution space of parato front representing different trade of among accuracy complexity and FLOPs of the network model. Generalized Normal Distribution parameters are involved in the Optimization process to get the less FLOPs without compromising the acceptable accuracy. The optimization problem for getting remarkable accuracy with minimum FLOPs can be derived as:

$$\underbrace{\min \text{FLOPs}\left(\vartheta_i^{(k)}\right)}_{\vartheta} = 2\sum_{9=1}^{K} \text{OFM}_{\text{height}} \times \text{OFM}_{\text{weight}} \times \text{ch}_{\text{in}} \times K \times k \times \text{ch}_{\text{out}} \quad (5)$$

Subject to $\varphi 1$

where Ĺ is layer count.

This technique can fine-tune VGGNet model in limited resource environment without compromising the significant performance of the network.

Obj-3: Minimization of Loss

MOGONET approach is used to optimize the loss of VGGNet model, Loss function determines the gap between obtained predicted values from the true data values actually defined. Most widely used loss function used in VGGNet model is cross entropy function and can be expressed as follows:

$$\text{loss}\left(\vartheta_i^{(k)}\right) = \frac{1}{Z}\sum_{i=1}^{Z}\sum_{j=1}^{N} a_{i,j} \log\left(\tilde{a}_{i,j}(\vartheta)\right) \quad (6)$$

where, $\text{loss}\left(\vartheta_i^{(k)}\right)$ is a loss function, N is the number of classes $a_{i,j}$ is a label indicator and $\tilde{a}_{i,j}$ is the predicted probability Minimize the $\text{loss}\left(\vartheta_i^{(k)}\right)$ of VGGNet model using MOGNDO by considering all other objective functions too. For loss optimization,

$$\text{Obj-3} = \underbrace{\min \text{loss}\left(\vartheta_i^{(k)}\right)}_{\vartheta} \quad (7)$$

Overall optimization function will be as follows:

$$\text{Overall (obj)} = \underbrace{\max\left[acc\left(\vartheta_i^{(k)}\right)\right]}_{\vartheta}\underbrace{\min}_{\vartheta}\left[FLOPs\left(\vartheta_i^{(k)}, loss\left(\vartheta_i^{(k)}\right)\right)\right] \quad (8)$$

Note on objectives and optimization: The CNN is trained using backpropagation to minimize the binary cross-entropy loss. Accuracy is used as an evaluation objective in the outer-loop multi-objective search (for ranking and selection of candidate solutions), rather than as a differentiable training loss. Although accuracy and loss are correlated, they capture complementary aspects: accuracy reflects thresholded correctness, while cross-entropy loss reflects confidence and penalizes overconfident errors. FLOPs are computed analytically from layer shapes using the standard convolution

and dense-layer FLOPs formulas (Eqs. 3–4), and are used to guide resource-aware architecture selection (e.g., input resolution and filter configuration) before training each candidate.

Proposed algorithm

Multi-objective optimization processes involve many divergent objectives, in contrast to single-objective optimization, which encompasses accuracy, loss, model cost, and algorithm complexity while aiming to maximize network efficiency and performance. To assess a MOGNDO process coupled with the VGGNet CNN model, the objectives must be articulated initially, followed by the establishment of the GND and the construction of the optimization process. The suggested methodology incorporates the MOGNDO structure with the VGGNet framework to enhance its hyperparameter optimization. By amalgamating the MOGNDO with VGGNet framework, hyperparameters, and other variables of the VGGNet model utilized for image classification can be optimized. This technique enhances various conflicting objectives simultaneously, such as model accuracy, complexity, parameter count, computational cost, and memory usage, while also minimizing the time needed to train the model. The GND is utilized to produce and upgrade the solution space during the process of optimization. For the normal distribution, the probability density function can be defined as follows:

$$\delta\left(x|\alpha,\beta,\gamma\right)=\frac{\gamma}{2\beta 9\left(\frac{1}{\gamma}\right)}\exp\left(-\left(\frac{|x-\alpha|}{\beta}\right)\right)^{\gamma} \quad (9)$$

where α is mean distribution, β,γ are scale and shape parameter and Ĺ is a gamma function.

Results

This section evaluates the efficacy of the suggested approach utilizing performance metrics on the conjunctive eye dataset. These include tri-objective computations and classification issues. These utilities are employed to evaluate the proficiency of multi-objective optimizers in tackling nonconvex and chaotic problems [31–35].

Parameters settings

Implementation and reproducibility

All experiments were implemented in Python using TensorFlow/Keras for model training and OpenCV for image processing. Experiments were executed on an NVIDIA Tesla P100-PCIE GPU (16 GB). Unless otherwise stated, all models were initialized with ImageNet pre-trained weights and trained for 50 epochs using stochastic gradient descent (momentum 0.9), batch size 64, sigmoid output activation, and learning rate 0.001 (Table 3). Baseline networks (VGG16, VGG19, ResNet18, ResNet50, and DenseNet) were trained with the same optimizer, learning rate, batch size, and number of epochs to ensure a fair comparison; only the architecture differs. Results are reported from a single run on a fixed train/validation/test split with a fixed random seed for data splitting and model initialization; therefore, small differences should be interpreted as comparable unless validated with repeated runs.

Evaluation metrics

We evaluate classification performance on the held-out test set using accuracy, precision, recall, and F1-score. In addition, we report binary cross-entropy loss and resource metrics (FLOPs and number of parameters) to quantify computational cost for deployment-oriented assessment.

For completeness, precision/recall/F1 are reported for the ablation study and the final proposed model (Table 6). Per-class metrics for all baselines can be reproduced using the released evaluation script on the same fixed split.

- Accuracy is computed to assess the efficacy of the optimized model. It quantifies the ratio of accurately predicted cases to the total instances in the evaluation set.
- Precision, recall, and F1-score are computed for the conjunctivitis (positive) class, using a decision threshold of 0.5. Precision = TP/(TP+FP), recall = TP/(TP+FN), and F1 = 2·(precision·recall)/(precision+recall).
- Floating-point operations serve as a criterion for assessing the computing effectiveness of a framework. FLOPs quantify the total arithmetic operations involving floating-point integers executed by a system.
- The loss function that quantifies the discrepancy between an expected likelihood and the corresponding label representing the actual category is termed the cross-entropy loss function. Reducing the loss function can lead to accuracy improvement in the prediction model by restricting the disparity of the identifying result.
- To examine the resource requirement of the network, several parameters can be computed. The parameter count directly affects the size of the model. It represents the adjustable biases and

weights to produce the estimate from the given information of the network.

Table 4 presents the experimental results on the conjunctivitis eye images. The objective is to validate the efficiency of the MOGONET by concerning the correctness deviations, among the baseline model and the optimized model underneath a static restraint. Diverse FLOPs and loss values are measured, and the number of parameters for both the original and optimized models is stated. The results indicate that MOGONET substantially decreases FLOPs, loss, and parameters while simultaneously enhancing accuracy. Utilizing the VGG-16 model can lead to a 57.82% reduction in FLOPs, as shown in Table 5. A variable quantity of filters is pruned from each convolutional layer, ranging from 311.53 to 57.84. Notwithstanding the substantial fall in FLOPs, accuracy has diminished by 1%, but loss has decreased by 53.56%. The number of parameters has decreased by 80%, from 15 million to roughly 3 million. Applying the VGG-19 model can result in a 65.17% reduction in FLOPs. In this instance, there has been a decline in FLOPs; accuracy has risen by 0.3%, while loss has diminished by 37.68%. The number of parameters has decreased from 20 million to 9 million, resulting in a 55% reduction. ResNet 50 model with MOO results in a 58.6% reduction in FLOPs. Despite the significant decrease in FLOPs, there has been a 0.35% drop in accuracy and a 72.98% reduction in loss. The number of parameters is reduced from 23 million to 11 million, indicating a 52.17% decrease. Employing the DenseNet model can result in a 55.98% decrease in FLOPs. Despite the substantial fall in FLOPs, accuracy has diminished by 0.35%, and loss has decreased by 51.98%. The number of parameters has decreased from 2 million to 0.2 million, signifying a 90% reduction. ResNet-18 with the MOO model results in a 78.77% reduction in FLOPs.

Considering the substantial fall in FLOPs, accuracy has improved by 0.61%, while loss has diminished by 37.85%. Decrease in the number of parameters from 12 million to 8 million, indicating a reduction of 33.33%. The results indicate that the MOGONET successfully optimized the VGGNet network through eliminating extraneous filters even though preserving those linked to discriminative features. This proposed method facilitates the decrease in parameters while preserving an adequate accuracy level. Table 5 presents the quantity of filters in both the original and optimized iterations of the proposed model, adhering to a 79.18% FLOPs reduction. It is apparent that all convolutional layers incorporate filters that are considered. Regarding the considerable fall in FLOPs, accuracy has improved by 1.5%, and loss has diminished by 91.14%. Decrease in the number of parameters from 9 million to 2 million, reflecting a reduction of 77.78%.

To produce more scalable, robust, and efficient outcome, the model can be fine-tuned using multi objective optimization across different input sizes of the image samples of conjunctivitis by balancing the other metrics like speed, resource requirement and accuracy. Applying multi objective optimization on varying input sizes can directly influence model efficiency. We train the proposed model using dynamic input resizing with multi-scale input like 100 × 100, 128 × 128, 256 × 256, and 512 × 512. Table 6 evaluated the tradeoff between accuracy with larger input and more computational cost.

The analysis is done over five distinct cases, as illustrated in Table 6. Cases 1 and 2, differing solely in the implementation of pre-processing, exhibit a noteworthy tendency. Case 1 attained 79.88%, and accuracy 81.49% is achieved by case 2, although the marginal enhancement in precision and recall in case 2 suggests that pre-processing enhances the system's capacity to accurately recognize real instances, despite not affecting the whole accurateness. The decrease in loss from 0.4732 to 0.3571 strengthens the idea that pre-processing improves the model's generalization capabilities by refining and regulating the data provided, thus slightly improving its learning efficiency.

Case 3 implements augmentation in addition to pre-processing, resulting in a substantial enhancement in outcomes: accuracy increases to 87.68%, precision to 88.37%, recall to 88.66%, and F-score to 85.57%. The significant reduction in loss to 0.1360 highlights the efficacy of image augmentation in developing additional resilient and comprehensive model. Image augmentation enhances the training dataset artificially, enabling the model to learn from a wider array of samples, so markedly enhancing its diagnostic proficiency. Case 4, which includes pre-processing, data augmentation, and segmentation via multi-thresholding, has superior performance across all measures, achieving notable accuracy (94.11%), precision (94.08%), recall (93.64%), and F-score (92.18%). The loss is reduced to a remarkable 0.0937, signifying an excellent alignment of the model with the data. This case underscores the collaborative impact of integrating all three strategies, with segmentation serving a

crucial function. Segmentation isolates regions of interest in images, ensuring the model concentrates on the most pertinent identifying traits, hence significantly improving its efficacy.

The significant disparity in outcome measures between 3 and 4 cases underscores the essential importance of segmentation in digital imaging chores. The incorporation of segmentation seems to enhance the model's capabilities, refining its focus and markedly decreasing the error rate. This indicates that although pre-processing and augmentation significantly enhance efficiency, segmentation is essential for attaining optimal accuracy and reliability in diagnoses. Case 5, which includes pre-processing, data augmentation, and segmentation by multi-thresholding and multi-objective optimization, demonstrates superior performance across all measures, achieving notable accuracy (98.32%), precision (97.54%), recall (96.92%), and F-score (96.22%). The loss is reduced to a remarkable 0.0193, signifying an excellent arrangement of the framework with the image samples. This case underscores the synergistic impact of integrating all three strategies, with MOO optimization serving a crucial function. The MOGND guarantees that the model prioritizes the most pertinent features for diagnosis, significantly improving its efficacy. Figure 6 illustrates the training and validation curves for accuracy and loss of the proposed MOGONET model.

The work establishes significant insights by providing a foundation for ongoing research in this domain. It focused on the practical applications of artificial intelligence in the medical sector, resulting in a relatively transformational change, and aims to augment the current body of knowledge in this domain. It is believed that all progressive development in utilizing expertise to tackle relevant medical concerns is essential. Significant comprehension is provided to examine the conjunctive ocular diseases by using DL and optimization techniques. The need for enhancement in the efforts is recognized, particularly with the expansion of datasets. Nonetheless, the real-world implication of the proposed study remains unaltered. The study significantly contributes to the research community by elucidating the diagnostic landscape of conjunctive eye illness over the investigation of contaminated pictures. Remarkable advancement is provided in the healthcare sector by indicating the prospective of DL to recognize critical ocular disorders. This research initiates a baseline for further improvement of image-based diagnostics for illnesses, helping in the global fight against disorders such as conjunctivitis in the future.

Discussion

Interpretation of results

The multi-objective search identifies Pareto-optimal configurations that balance predictive performance with computational cost. Across the evaluated CNNs, MOGONET substantially reduces FLOPs and parameters while maintaining competitive accuracy, indicating that over-parameterization can be reduced for this task without major loss of discriminative ability.

Why optimize both accuracy and loss

Accuracy is a thresholded metric and can remain unchanged while confidence shifts. Cross-entropy loss provides a smoother signal that penalizes overconfident misclassifications and helps distinguish models with similar accuracy but different calibration and margin. Optimizing both objectives improves the stability of selection when accuracy differences are small.

Role of pre-processing, augmentation, and segmentation

The ablation study (Table 6) shows that adding augmentation improves generalization relative to pre-processing alone, and segmentation further boosts performance by emphasizing conjunctival regions and suppressing background noise. Combining these steps with multi-objective optimization yields the best trade-off between accuracy and efficiency.

FLOPs estimation and practical efficiency

FLOPs were computed analytically from layer shapes, enabling fast evaluation of candidate architectures during the search. The resulting reductions translate to faster inference and lower energy usage on constrained hardware, which is important for screening tools deployed on edge devices or in low-resource settings.

Future work

Future studies should validate the approach on clinically curated datasets with patient-level splits, report mean ± std over multiple runs, and analyze robustness across imaging conditions (illumination, device type) to better support real-world deployment.

Limitations and validity

The dataset is assembled from web sources and may contain acquisition bias, near-duplicates, and label noise. Although we applied duplicate screening and group-wise splitting to reduce leakage, results are reported from a single run on a fixed split; therefore, small differences between methods should be treated as comparable unless confirmed across multiple seeds or cross-validation. Additionally, labels are based on dataset annotations and are not clinically verified.

Conclusion

This paper presented MOGONET, a multi-objective optimization framework for conjunctivitis screening from conjunctival eye images. The proposed pipeline combines image enhancement CLAHE, augmentation, and multi-level thresholding–based segmentation with TL using a VGG-based backbone. MOGONET performs an outer-loop multi-objective search to identify efficient model configurations that balance accuracy, loss, and computational cost FLOPs.

Overall, the optimized MOGONET configuration achieves 98.32% test accuracy while reducing FLOPs by 79.18% and parameters from approximately 9 M–2 M (77.78% reduction), compared with the unoptimized VGG-based model. These results suggest that resource-aware optimization can substantially simplify CNN models for conjunctivitis classification without sacrificing performance. Because results are reported from a single run on a fixed split and the dataset is web-sourced, future work should confirm robustness across multiple random seeds and clinically curated datasets.

Future research initiatives involve broadening the dataset to encompass a wider range of ocular disorders and integrating supplementary pre-processing and methods to improve model efficacy. Investigating alternative DL structures, and may yield avenues for enhancement. Moreover, the incorporation of MOGONet into practical clinical processes and its evaluation across various healthcare environments would be crucial to properly harness its potential advantages for helping patients.

Author contributions

All authors contributed to the study conception and design, data preparation, experiments, analysis and interpretation of results, and manuscript writing and revision. All authors reviewed and approved the final manuscript.

References

1. Kasiviswanathan S, Bai Vijayan T, Simone L, Dimauro G. Semantic segmentation of conjunctiva region for non-invasive anemia detection applications. Electronics 2020; 9(8):1309.
2. A. Azari A, Arabi A. Conjunctivitis: a systematic review. J Ophthalmic Vis Res 2020; 15(3):372–95.
3. Cameron L, Rueda A. Infectious Diseases: common Outpatient Considerations. In: Pediatric Rotations: a Quick Guide for Medical Students Springer International Publishing, Cham, Switzerland, p 311, 2024.
4. Deng X, He D, Qu L. A novel hybrid algorithm based on arithmetic optimization algorithm and particle swarm optimization for global optimization problems. J Supercomput 2024; 80(7):8857–97.
5. Zhang Y, Jin Z, Mirjalili S. Generalized normal distribution optimization and its applications in parameter extraction of photovoltaic models. Energy Convers Manag 2020; 224:113301.
6. Shalihin MS, Asri NA. Audit of ophthalmological case management: a case series review at a local health clinic. Asian J Med Health Sci 2024; 7(2):248.
7. Yu L, Xu H, Jiang Z, Yang H, Cui Y, Li Y. Comorbidity of physical illnesses and mental disorders in outpatients with tic disorders: a retrospective study using the outpatient case system. Front Neurol 2024; 15:1397766.
8. Bielory L, Delgado L, Katelaris CH, Leonardi A, Rosario N, Vichyanoud P. ICON: diagnosis and management of allergic conjunctivitis. Ann Allergy Asthma Immunol 2020; 124(2):118–34.
9. Frost HM, Jenkins TC, Meece JC, Savor-Price C, Wilson ML, Keith A, et al. Etiology and outcomes of acute infectious conjunctivitis in children. J Pediatr 2025; 276:114368.
10. Gamil S, Zeng F, Alrifaey M, Asim M, Ahmad N. An efficient AdaBoost algorithm for enhancing skin cancer detection and classification. Algorithms 2024; 17(8):353.
11. Kurtansky NR, D'Alessandro BM, Gillis MC, Betz-Stablein B, Cerminara SE, Garcia R, et al. The SLICE-3D dataset: 400,000 skin lesion image crops extracted from 3D TBP for skin cancer detection. Sci Data 2024; 11(1):884.
12. Patel SK, Wekalao J, Mandela N, Al-Zahrani FA. Design of encoded graphene-gold metasurface-based circular ring and square sensors for brain tumor detection and optimization using XGBoost algorithm. Diam Relat Mater 2024; 148:111439.
13. Abdulahi AT, Ogundokun RO, Adenike AR, Shah MA, Ahmed YK. PulmoNet: a novel deep learning based pulmonary diseases detection model. BMC Med Imag 2024; 24(1):51.
14. Dhiman P, Choudhary A, Wadhwa S, Kaur A. Improving deep learning classifiers performance using preprocessing and cycle scheduling approaches in a plant disease detection. In 2024

11th International Conference on Reliability, Infocom Technologies and Optimization (ICRITO), 2024, pp. 1–5.
15. Dhiman P, Wadhwa S, Choudhary A, Kaur A, Malra K. DERMONET: lightweight diagnostic system for dermatological conditions using SqueezeNet framework. [Unpublished manuscript].
16. Pahwa S, Kaur A. VNCESM: vGG-Net based conjunctive eyes segmentation model with transfer learning. In 2024 11th International Conference on Reliability, Infocom Technologies and Optimization (ICRITO), IEEE, Noida, India, 2024, p. 1–5.
17. Alanazi TA, Albuainain A, AlKhaldi HM, Al-Abdulqader RA, Aldosari NH. Keratoconus and macular corneal dystrophy simultaneous presentation with an exacerbation after an upper respiratory infection of COVID-19 and viral conjunctivitis. Bahrain Med Bull 2023; 45(2):1510.
18. Anand SK, Kumar S. Uncertainty analysis in ontology-based knowledge representation. New Gener Comput 2022; 40(1):339–76.
19. Khan A, Deb K. Optimizing keyboard configuration using single and multi-objective evolutionary algorithms. In Proceedings of the Companion Conference on Genetic and Evolutionary Computation, 2023, pp. 219–22.
20. Mokabberi A, Golsorkhtabari M, Varzi RA. Proposing an advanced trending-based grey wolf optimizer for single-objective optimization problems. In 20th CSI International Symposium on Artificial Intelligence and Signal Processing (AISP), 2024, p. 1–7.
21. Cenikj G, Petelin G, Eftimov T. TransOptAS: transformer-based algorithm selection for single-objective optimization. In Proceedings of the Genetic and Evolutionary Computation Conference Companion, 2024, pp. 403–6.
22. Omid A, Azar A, Taleb M. Assessing environmental and operational efficiencies: a multi-objective optimization problem in a two-stage network data envelopment analysis. IMA J Manag Math 2024; 35(4):693–713.
23. Conjunctivitis Dataset. Kaggle. Available via https://www.kaggle.com/datasets/alisofiya/conjunctivitis/(Accessed 16 October 2023).
24. Conjunctivitis Images. Shutterstock. Available via https://www.shutterstock.com/search/conjunctivitis/ (Accessed 25 October 2023).
25. Seelwal P, Dhiman P, Gulzar Y, Kaur A, Wadhwa S, Onn CW. A systematic review of deep learning applications for rice disease diagnosis: current trends and future directions. Front Comput Sci 2024; 6:1452961.
26. Pahwa S, Kaur A, Dhiman P, Damasevičius R. ConjunctiveNet: an improved deep learning-based conjunctive-eyes segmentation and severity detection model. Int J Intell Comput Cybern 2024; 17(4):783–804.
27. Cirik E, Osman O, Esen V. Exploring the impact of CLAHE processing on disease classes in the NIH Chest X-Ray dataset using VGG16 and ResNet50 architectures. International Conference on Forthcoming Networks and Sustainability in the AIoT Era, Springer Nature Switzerland, Cham, Switzerland, pp 422–9, 2024.
28. Gharehchopogh FS, Ibrikci T. An improved African vultures optimization algorithm using different fitness functions for multi-level thresholding image segmentation. Multimed Tools Appl 2024; 83(6):16929–75.
29. Kaushal C. Monkeypox and other skin conditions detection utilizing CNN with VGG16 transferred language. In Proceedings of the 2023 6th International Conference on Contemporary Computing and Informatics (IC3I), IEEE, 2023, 6, pp. 931–8.
30. Khodadadi N, Khodadadi E, Abdollahzadeh B, Ei-Kenawy ESM, Mardanpour P, Zhao W, et al. Multi-objective generalized normal distribution optimization: a novel algorithm for multi-objective problems. Clust Comput 2024; 27:1–43.
31. Zhang Y. An improved generalized normal distribution optimization and its applications in numerical problems and engineering design problems. Artif Intell Rev 2023; 56(1):685–747.
32. Yasmin F, Hassan MM, Hasan M, Zaman S, Kaushal C, El-Shafai W, et al. PoxNet22: a fine-tuned model for the classification of monkeypox disease using transfer learning. IEEE Access 2023; 11:24053–76.
33. Tymchenko B, Marchenko P, Spodarets D. Deep learning approach to diabetic retinopathy detection. arXiv. 2020:arXiv:2003.02261.
34. Imran M, Ullah A, Arif M, Noor R. A unified technique for entropy enhancement based diabetic retinopathy detection using hybrid neural network. Comput Biol Med 2022; 145:105424.
35. Jeny AA, Junayed MS, Islam MB. Deep neural network-based ensemble model for eye diseases detection and classification. Image Anal Stereol 2023; 42(2):77–91.